Baek et al., Supplemental Figure 1.

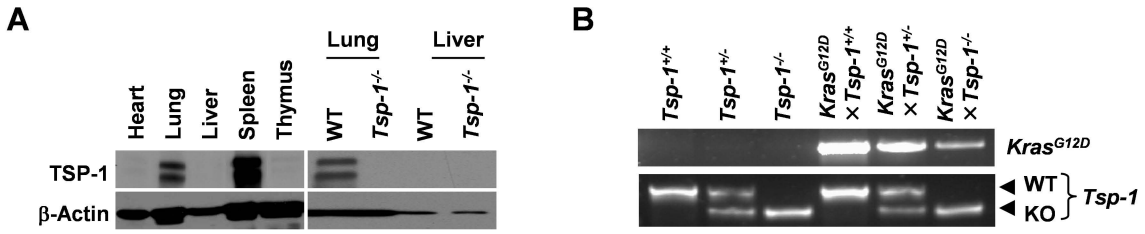

Figure S1. Generation of conditional *LSL-Kras^{G12D}* mice with *Tsp-1*-null background. (**A**) Tissues were harvested from wild-type mice and assessed for TSP-1 expression by immunoblotting. Liver and lung tissues from *Tsp-1$^{-/-}$* mice were used as negative controls. (**B**) Representative *LSL-Kras^{G12D}* × *Tsp-1$^{-/-}$* genotyping.

Baek et al., Supplemental Figure 2.

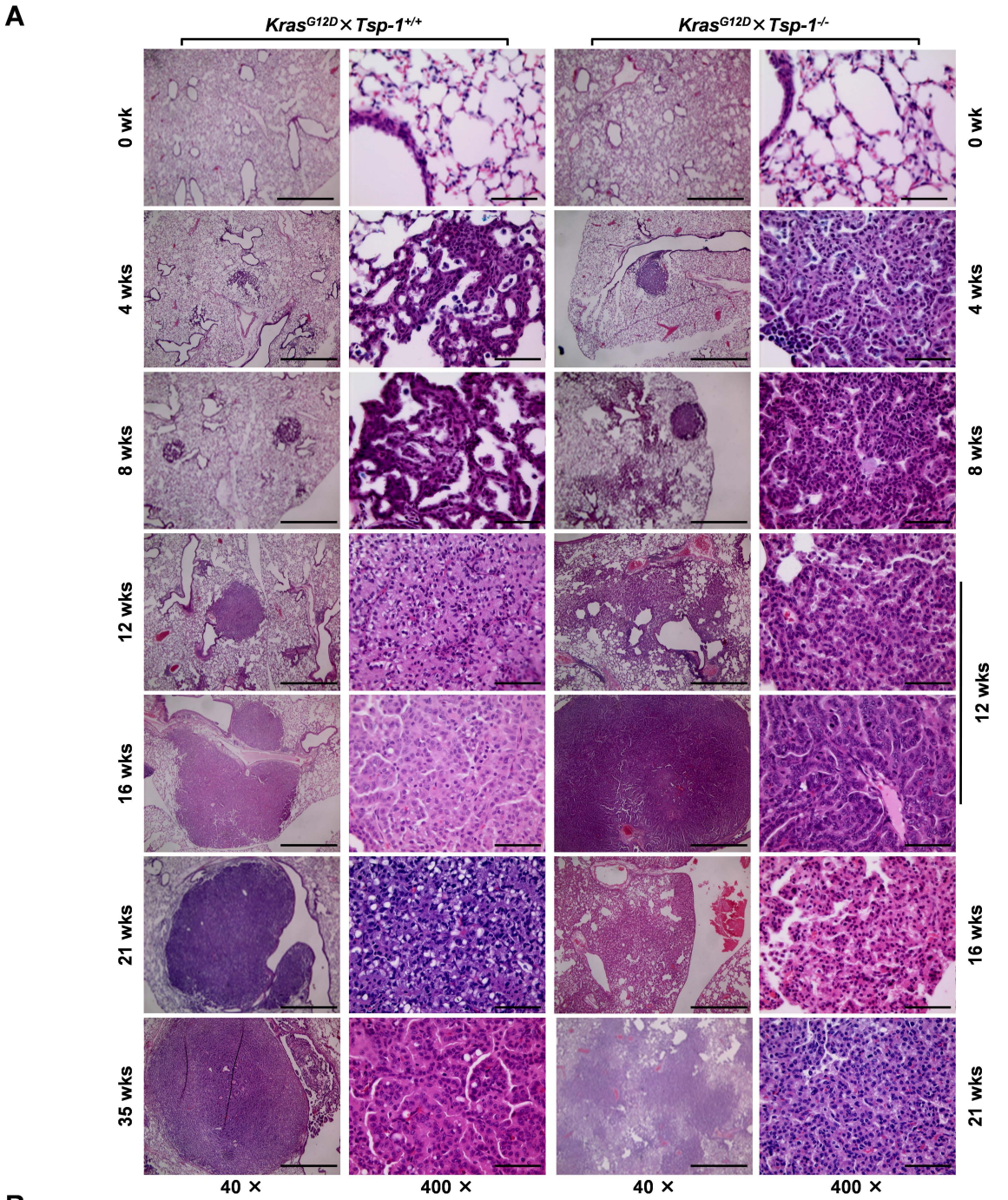

Figure S2. Loss of TSP-1 accelerates lung tumor progression driven by oncogenic *Kras*. (**A** and **B**) Time-course analysis of lung tumor progression in *LSL-Kras*^{G12D}×*Tsp-1*$^{+/+}$ and *LSL-Kras*^{G12D}×*Tsp-1*$^{-/-}$ mice. Lungs from 4 to 10 mice per each group were harvested at the indicated times after oncogenic *Kras*^{G12D} activation. Histopathological analysis of lung lesions was performed on H&E-stained sections. AAH and EH indicate atypical adenomatous hyperplasia and epithelial hyperplasia, respectively. Scale bars: 1 mm (40×); 50 μm (400×).

Baek et al., Supplemental Figure 3.

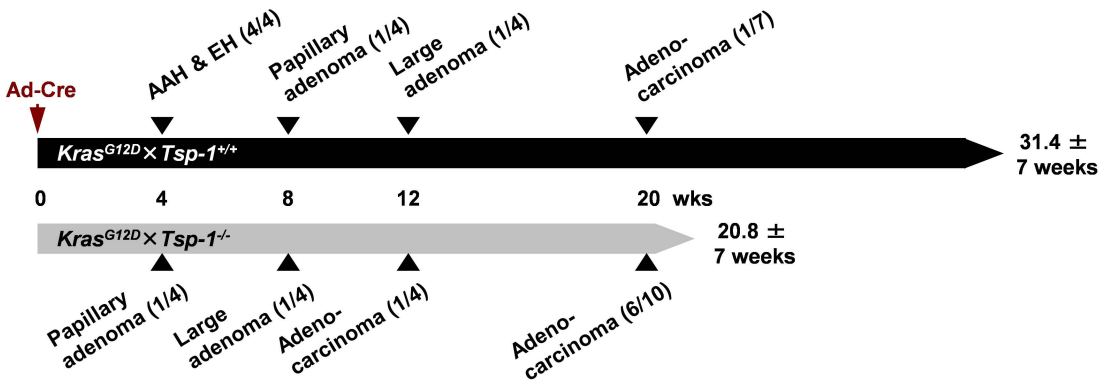

Figure S3. Schematic diagram of time line of *Kras*^{G12D}-mediated lung tumor progression on a *Tsp-1*$^{+/+}$ and *Tsp-1*$^{-/-}$ mice. Ratios indicate the number of mice with corresponding lesions compared to the total number of mice examined.

Baek et al., Supplemental Figure 4.

A

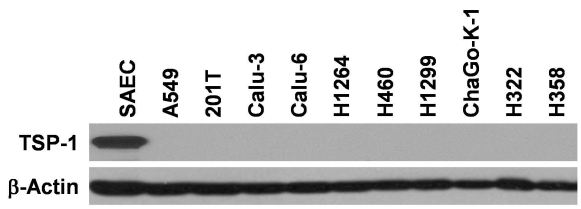

B

Cell Line	K-ras status	p53 status
A549	mutant	WT
H460	mutant	WT
H1264	mutant	mutant
H1299	WT	null
H358	mutant	null
H322	WT	mutant
Calu-3	mutant	mutant
Calu-6	mutant	null
ChaGo-K-1	mutant	WT
201T	mutant	WT

Figure S4. TSP-1 expression is dramatically downregulated in human adenocarcinoma cells. (**A**) TSP-1 expression in 10 different human lung adenocarcinoma cell lines was assessed by immunoblotting. Normal small epithelial airway cells (SAEC) was used as a positive control for TSP-1 expression. β-Actin was probed as a loading control. (**B**) *Kras* and *p53* status in human adenocarcinoma cell lines used in the study.

Baek et al., Supplemental Figure 5.

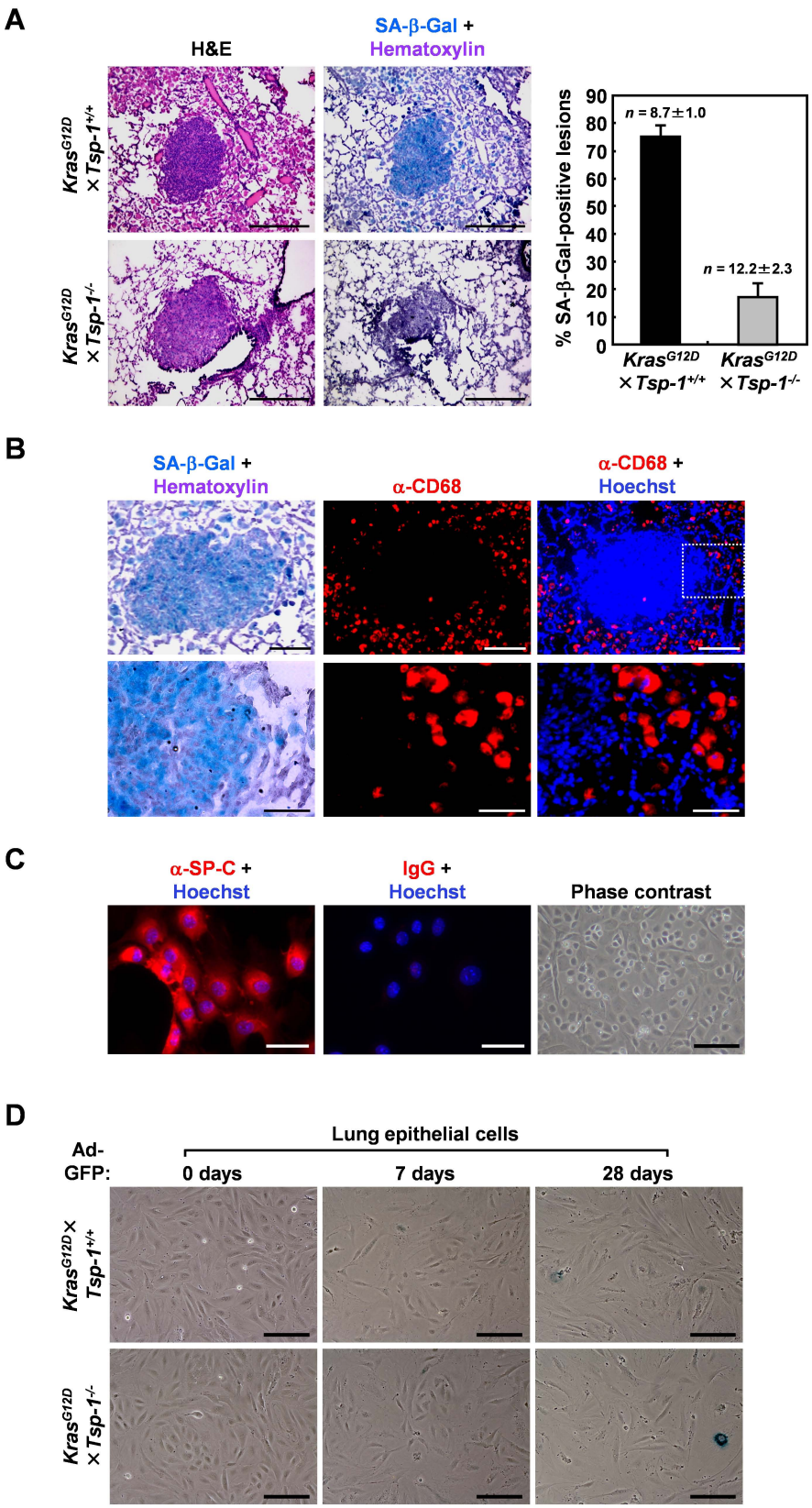

Figure S5. Oncogenic *Ras*-induced senescence is compromised in the absence of TSP-1. (**A**). Lung tumors were harvested from *LSL-Kras*^{G12D}×*Tsp-1*$^{+/+}$ and *LSL-K-ras*^{G12D}×*Tsp-1*$^{-/-}$ mice (n=6 per group) at 21 weeks post-Ad-Cre infection and stained for SA-β-Gal activity. The number of SA-β-Gal-positive lesions was quantified relative to the total number of lesions. The average number of adenomatous lesions counted per mouse is indicated above the error bar and data are represented as mean ± SEM. Scale bars: 200 μm. (**B**) SA-β-Gal positive lung tumor lesions were immunostained for CD68, a macrophage marker, to discriminate SA-β-Gal-positive tumor cells from infiltrating macrophages. Scale bars: 200 μm (*upper*); 50 mm (*lower*). (**C**) Primary lung epithelial cells were isolated and their identity was confirmed by immunostaining for the lung epithelial cell specific marker, SP-C. Scale bars: 50 μm. (**D**) Primary adult lung epithelial cells isolated from *LSL-Kras*^{G12D}×*Tsp-1*$^{+/+}$ and *LSL-K-ras*^{G12D}×*Tsp-1*$^{-/-}$ mice were assessed for SA-β-Gal positivity on the indicated days after infection with Ad-GFP as a negative control for *Kras*^{G12D}-induced senescence upon Ad-Cre infection. Scale bars: 200 μm.

Baek et al., Supplemental Figure 6.

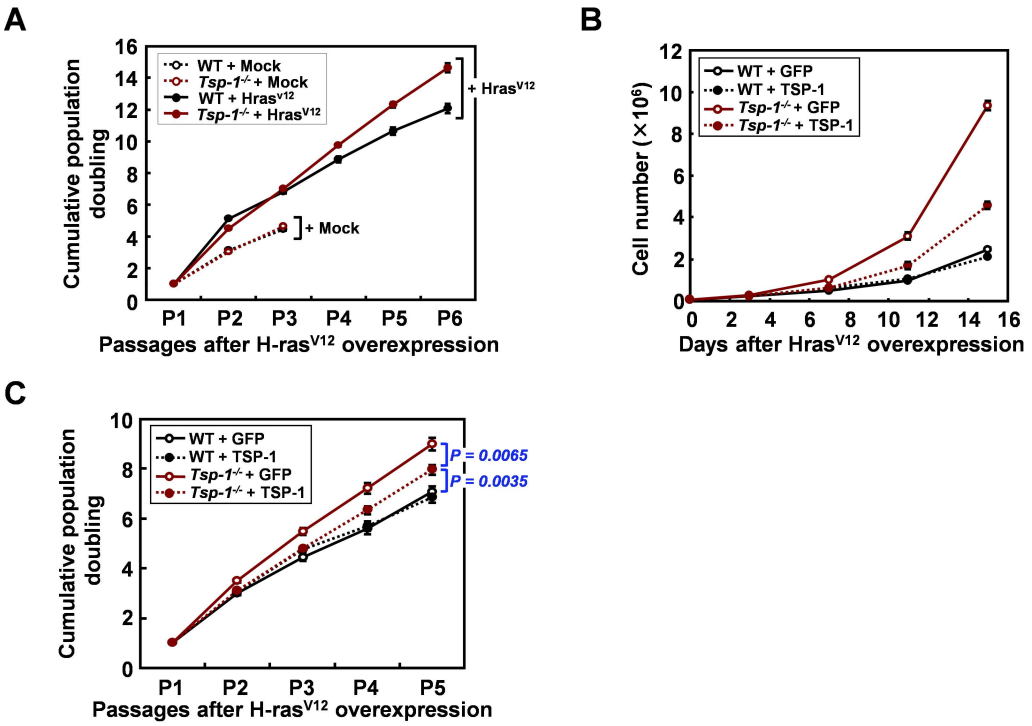

Figure S6. Ectopic expression of TSP-1 reduces oncogenic *Hras*-induced cell proliferation. (**A**) Cumulative population doublings of WT and *Tsp-1*$^{-/-}$ lung fibroblasts upon Hras^{V12} expression *in vitro*. (**B** and **C**) Proliferation (B) and cumulative population doubling (C) of WT and *Tsp-1*$^{-/-}$ lung fibroblasts expressing TSP-1 or GFP was measured after *Hras*^{V12} expression. Data are represented as mean ± SEM.

Baek et al., Supplemental Figure 7.

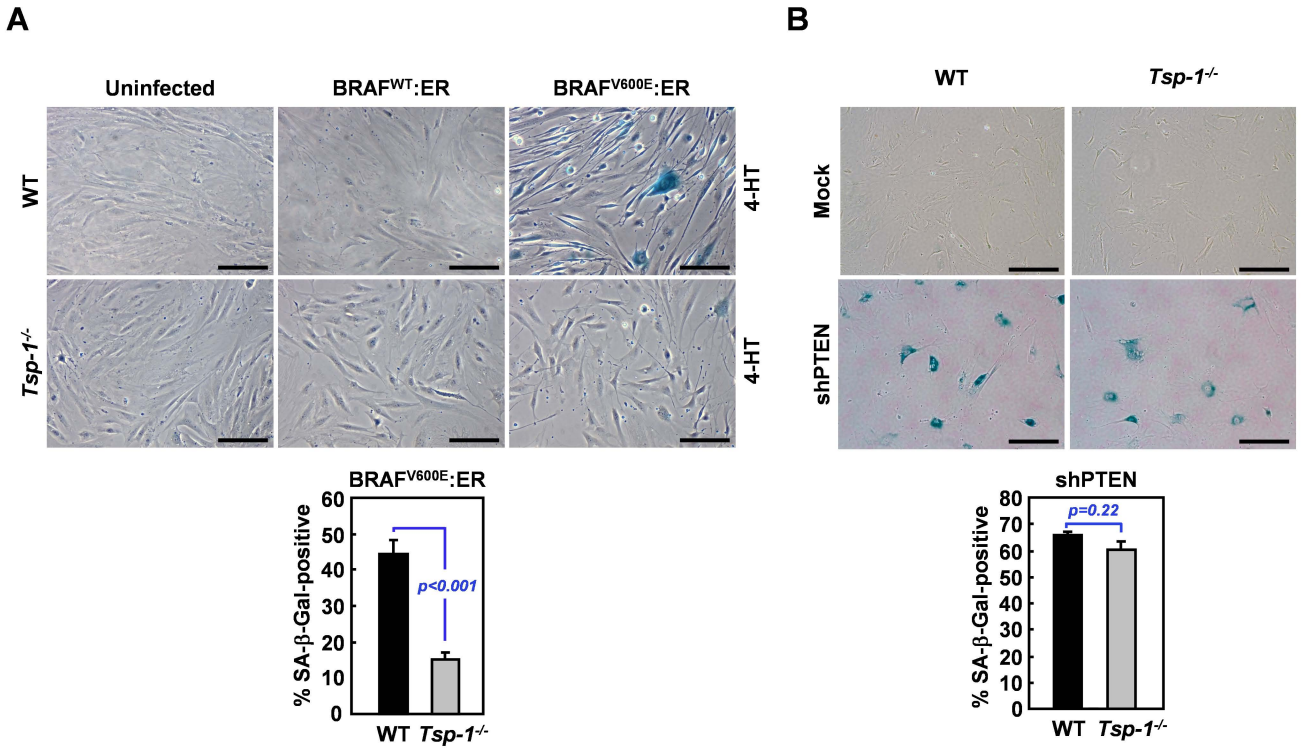

Figure S7. Loss of TSP-1 abrogates premature senescence in primary lung fibroblasts induced by oncogenic *Braf* but not by PTEN depletion. (**A**) Senescence of WT and *Tsp-1*$^{-/-}$ lung fibroblasts induced by *Braf*^{V600E} expression. Cells were retrovirally infected with Braf^{WT}:ER or Braf^{V600E}:ER, treated with 100 nM 4-hydroxytamoxifen (4-HT) for 14 days, and stained for SA-β-Gal activity. (**B**) Senescence induced by PTEN loss was assessed in primary adult lung fibroblasts from WT and *Tsp-1*$^{-/-}$ mice. Cells were infected with a retroviral PTEN shRNA and 11 days later examined for SA-β-Gal activity. Data are represented as mean ± SEM. Scale bars: 200 μm.

Baek et al., Supplemental Figure 8.

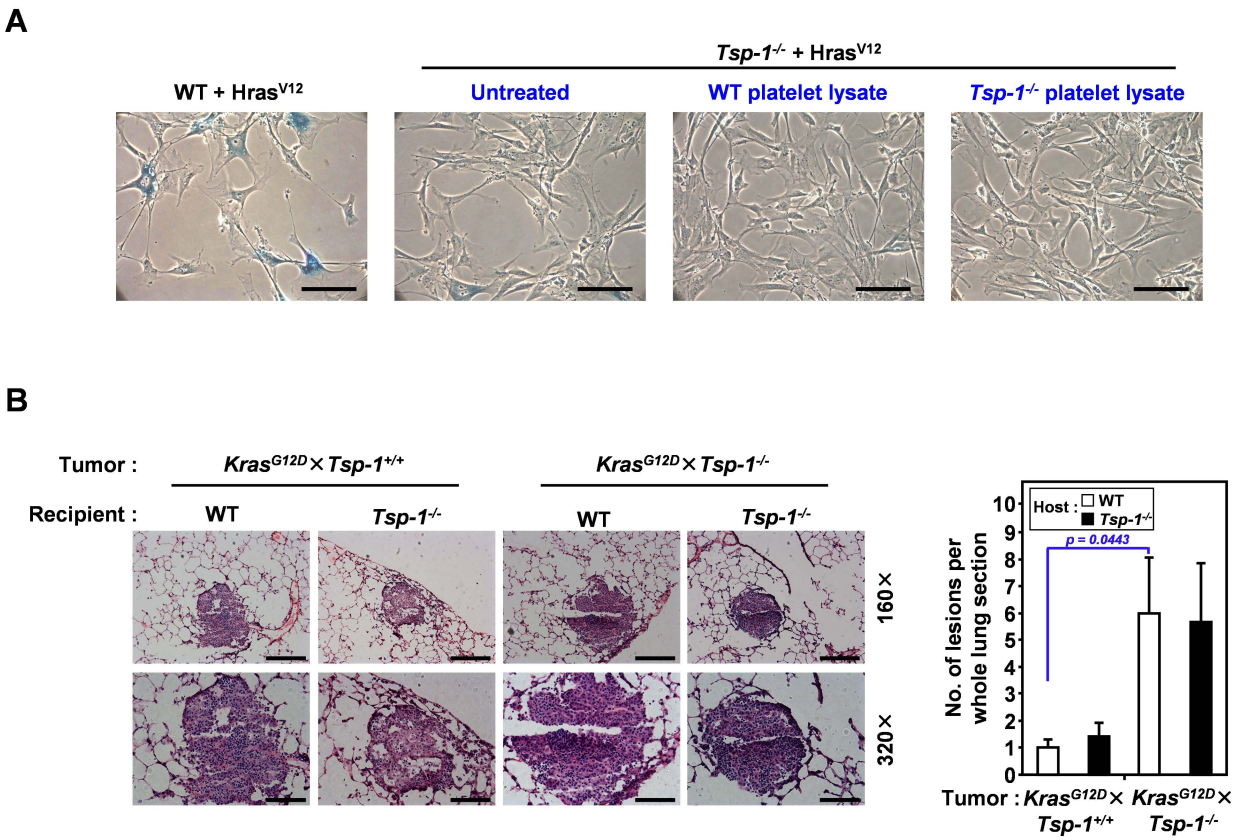

Figure S8. Extracellular TSP-1 does not rescue oncogenic Ras-induced senescence in *Tsp-1*$^{-/-}$ lung fibroblasts and tumor cells. (**A**) 10^8 platelets isolated from wild-type or *Tsp-1*$^{-/-}$ mice lysed in PBS containing 1 U/ml thrombin at 37°C for 10 min, diluted in 2 ml of culture media, and used for the treatment of lung fibroblasts. 5 × 10^4 *Tsp-1*$^{-/-}$ lung fibroblasts retrovirally transduced with *Hras*^{V12} were plated in 6 well tissue culture plates, treated with platelet lysates every other day up to 16 days, and stained for SA-β-Gal positivity to visualize senescent cells. Wild-type fibroblasts expressing Hras^{V12} were used as a positive control. Scale bar: 200 μm. (**B**) Large lung adenomas were dissected from *Kras*^{G12D}*Tsp-1*$^{+/+}$ and *Kras*^{G12D}*Tsp-1*$^{-/-}$ mice at 20 weeks after intranasal instillation of Ad-Cre and dissociated with 2 mg/ml collagenase/dispase for 45 min at 37°C. Then 10^6 tumor cells were inoculated via tail vein injection into either wild-type or *Tsp-1*$^{-/-}$ mice (*n=5* per group). 38 days after tumor cell injection, lungs were harvested and stained with H&E for histological examination. Data are represented as mean ± SEM. Scale bar: 200 μm (160×); 100 μm (320×).

Baek et al., Supplemental Figure 9.

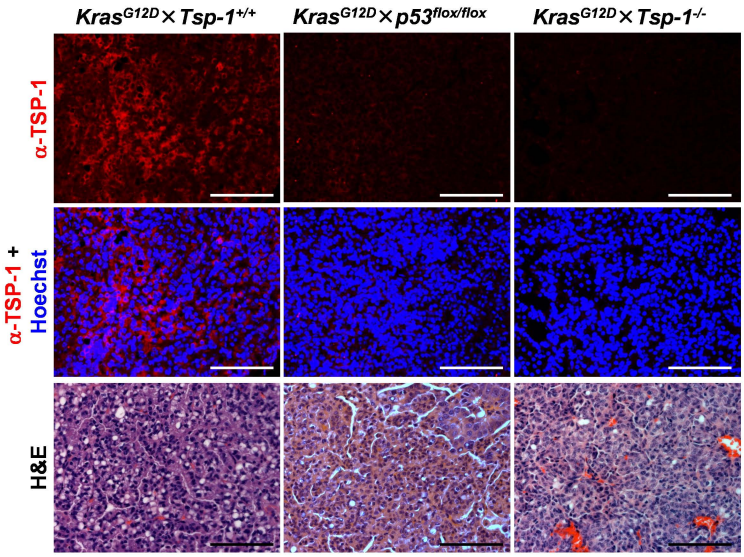

Figure S9. TSP-1 expression is significantly decreased in large lung adenomas depleted for *p53*. Large lung adenomas developed in *LSL-Kras^{G12D}×Tsp-1$^{+/+}$* and *LSL-Kras^{G12D}×p53$^{flox/flox}$* mice after Ad-Cre infection was assessed by immunofluorescence for TSP-1. Large lung adenomas from *LSL-Kras^{G12D}×Tsp-1$^{-/-}$* mice were also stained for TSP-1 as negative controls. Scale bars: 100 μm.

Baek et al., Supplemental Figure 10.

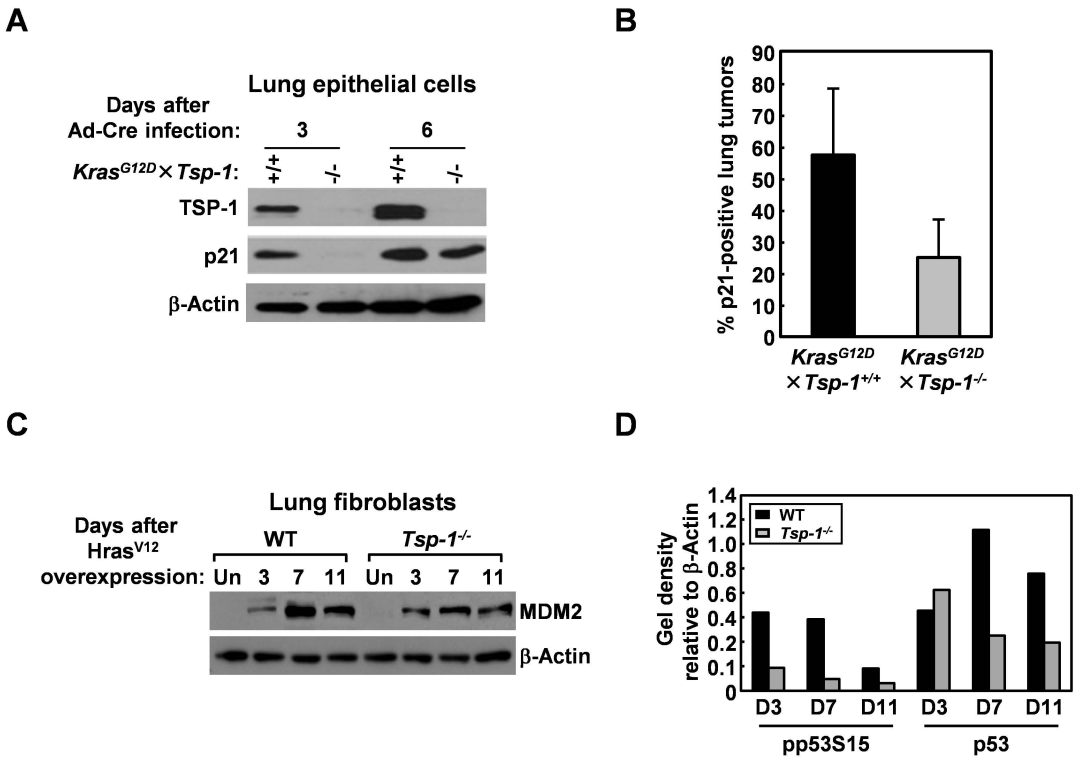

Figure S10. p53 and p21^{cip1} expression are decreased in the absence of TSP-1. (**A**) TSP-1 and p21^{cip1} expression in lung epithelial cells isolated from *LSL-Kras*^{G12D}×*Tsp-1*$^{+/+}$and *LSL-Kras*^{G12D}×*Tsp-1*$^{-/-}$ mice after Ad-Cre infection was assessed by immunoblotting. (**B**) p21^{cip1}-positive lung tumors were quantified in lungs from *LSL-Kras*^{G12D}×*Tsp-1*$^{+/+}$ and *LSL-Kras*^{G12D} ×*Tsp-1*$^{-/-}$ mice (*n=4* per group) at 21 weeks post-infection. Data are represented as mean ± SEM. (**C**) MDM2 expression was examined in WT and *Tsp-1*$^{-/-}$ lung fibroblasts at the indicated days after oncogenic *Hras* expression. β–Actin was probed as a loading control. (**D**) The relative gel densities of phospho-p53^{S15} in WT and *Tsp-1*$^{-/-}$ lung fibroblasts after oncogenic *Hras* expression at the indicated days were quantified by densitometry and normalized to total p53 levels.

Baek et al., Supplemental Figure 11.

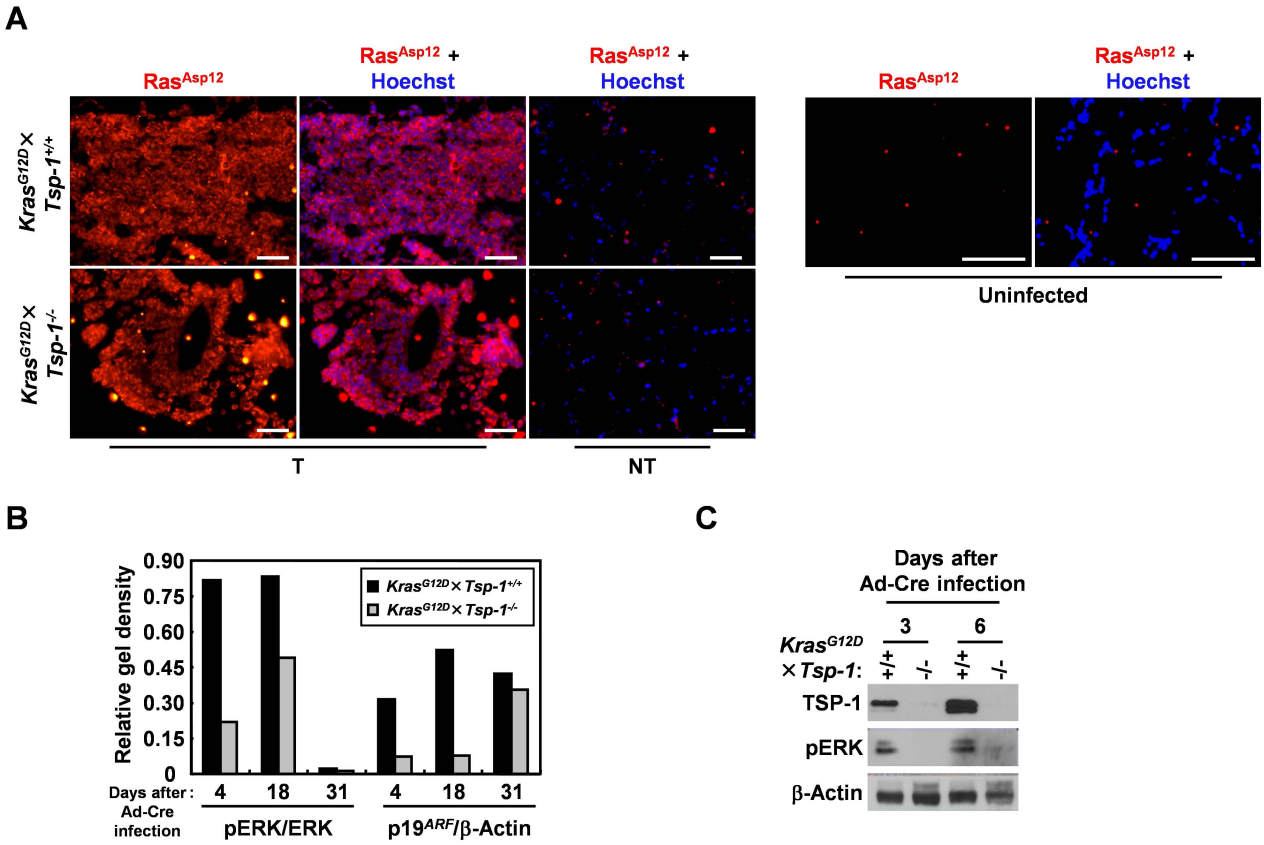

Figure S11. The activation of ERK and p19ARF induced by oncogenic *Kras* is attenuated in the absence of TSP-1. (**A**) Lungs were harvested at 21 weeks post-Ad-Cre infection from *LSL-Kras*^{G12D}×*Tsp-1*$^{+/+}$ and *LSL-Kras*^{G12D}×*Tsp-1*$^{-/-}$ mice and immunostained with an anti-Ras^{Asp12} antibody. T indicates tumor and NT indicates no tumor (*left panel*). Lungs from uninfected mice were also stained for Ras^{Asp12} as a negative control (*right panel*). Scale bars: 100 μm. (**B**) Expression of pERK and p19^{ARF} in lung fibroblasts harvested from *LSL-Kras*^{G12D}×*Tsp-1*$^{+/+}$ and *LSL-Kras*^{G12D}×*Tsp-1*$^{-/-}$ mice and treated with Ad-Cre *in vitro* at the indicated days were quantified by densitometry and normalized to total ERK and β-Actin, respectively. (**C**) Primary lung epithelial cells were isolated from *LSL-Kras*^{G12D}×*Tsp-1*$^{+/+}$ and *LSL-Kras*^{G12D}×*Tsp-1*$^{-/-}$ mice, infected with Ad-Cre *in vitro*, harvested at the indicated time points and probed for TSP-1, pERK, and β-Actin as a loading control.

Baek et al., Supplemental Figure 12.

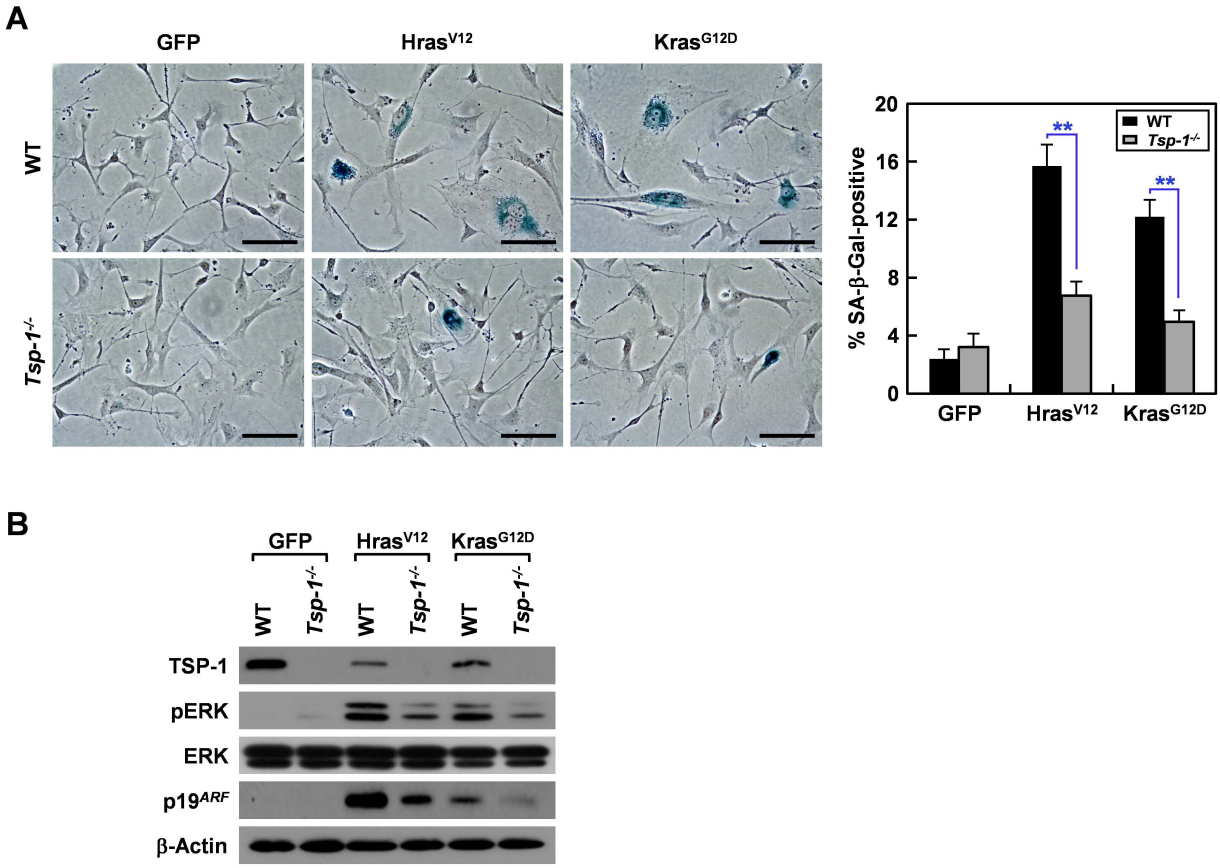

Figure S12. Loss of TSP-1 abrogates premature senescence in primary lung fibroblasts induced by oncogenic *Kras^{G12D}*. (**A**) Senescence of WT and *Tsp-1$^{-/-}$* lung fibroblasts induced by exogenous *Kras^{G12D}* expression. Cells were infected with lentiviruses expressing *Kras^{G12D}*, *Hras^{V12}* as a positive control or GFP as a negative control and stained for SA-β-Gal activity at 8 days after infection. Scale bars: 100 μm. Data are represented as mean ± SEM. ** $p < 0.01$. (**B**) Cells lentivirally infected with *Kras^{G12D}* , Hras^{V12} or GFP were harvested at 7 days after infection and probed for TSP-1, phosphoERK (pERK), total ERK, and p19^{ARF} expression by immunoblotting. β-Actin was probed as a loading control.